

Chapter 5 Continuing The Solar Neighborhood Census: Infrared Parallax Program At Fan Mountain Observatory

5.1 INTRODUCTION

Even in the well-surveyed northern hemisphere, only 1,153 stellar systems are identified as being within 25 parsecs (pc) out of an expected 2,750 systems (Henry *et al.* 2002). The known systems incorporate the bright nearby stars filled in by the Hipparcos Space Astrometry Mission (ESA 1997, hereafter Hipparcos). The Hipparcos catalog includes stars as faint as 12.4 magnitude in V-band ($V_{\text{Johnson-Morgan}}=550$ nm according to Johnson and Morgan 1951, 1953). However, it is significantly incomplete for stars fainter than 9 magnitude (Perryman *et al.* 1997); the 12.4 magnitude corresponds to an M5V star at approximately 10.5 pc, the 9 magnitude to a distance of about 2.2 pc (Drilling & Landolt 2000). Most of the missing systems must therefore consist of intrinsically faint stars and brown dwarfs; such cool objects will have their peak emission at wavelengths of 0.9 micrometers (μm) and longer (Drilling & Landolt 2000). As demonstrated in Chapter 4, infrared surveys, such as the Two Micron All Sky Survey (Skrutskie *et al.* 2006, hereafter 2MASS) and the Deep Near Infrared Survey of the Southern Sky (Epchtein *et al.* 1999, hereafter DENIS) are fertile sources of potential nearby stars.

These infrared surveys are also significant sources of brown dwarfs, which cool continuously because they lack sufficient mass to sustain nuclear fusion. Trigonometric parallaxes to these substellar objects would allow accurate determination of their luminosities. According to Chabrier and Baraffe (2000), most brown dwarf radii should be similar to that of Jupiter. Therefore, better luminosities would also improve

temperature estimates. Gelino, Kirkpatrick, and Burgasser (2004) list 581 likely L and T dwarfs of which only 75 have parallax measurements.¹⁵ As discussed in Chapter 4, the Cerro Tololo Inter-American Observatory Parallax Investigation (CTIOPI) includes some southern L dwarfs. However, all brown dwarfs within the reach of ground-based astrometry should have their distances measured, regardless of whether they lie within the immediate solar neighborhood.

From 2000 until 2006, the United States Naval Observatory (USNO) operated an infrared parallax program in Flagstaff, Arizona, using the 61-inch (1.55-meter) reflector and an astrometric, infrared detector known as ASTROCAM. In response to the need for brown dwarf parallax measurements, Vrba *et al.* published preliminary infrared parallaxes for 40 L and T dwarf in 2004; at the time, another two years of observations was anticipated in order to finalize them. Unfortunately, a Dewar explosion during a nearby forest fire in June 2006 destroyed ASTROCAM. The program will be suspended for at least a year and perhaps longer (F. Vrba 2006, private communication). Even when the USNO program was operating, a desire for an additional infrared parallax program to increase the number of brown dwarfs with such determinations was clear.

The University of Virginia (UVa) had long been a leader in the measurement of parallaxes with programs at Leander McCormick Observatory, Fan Mountain Observatory, and Siding Spring Observatory. However, the last of these,

¹⁵DwarfArchive.org maintains a list of late type stars at <http://spider.ipac.caltech.edu/staff/davy/ARCHIVE/> Counts reported herein were accurate as of 2006 October 16.

the UVa Southern Parallax Program at Siding Spring Observatory in Australia, discontinued observations in July 2002. Once the Virginia Astronomical Instrumentation Laboratory (VAIL) began development of an infrared camera for use at Fan Mountain Observatory, this study of the feasibility of a new parallax program was instigated. In addition, M. Skrutskie (2005, private communication) obtained 15 percent (%) of the time on the Fred Lawrence Whipple Observatory 1.3-meter telescope, which is now the Peters Automated Infrared Imaging Telescope (PAIRITEL) on Mount Hopkins in exchange for remounting the former 2MASS camera there. This allocation provides another possible opportunity for infrared astrometry at UVa.

5.2 FAN MOUNTAIN 31-INCH TELESCOPE

UVa operates Fan Mountain Observatory at a dark site approximately 19 miles (30 kilometers) south of Charlottesville, Virginia, in Covesville. Tinsley Laboratories built the 31-inch (0.8-meter) astrometric reflector in the 1960's for use with a photographic plate spectrograph and photomultipliers. In 2004, VAIL, led by Skrutskie, refurbished the telescope and outfitted it with a new infrared camera, FanCam.

VAIL designed and developed the infrared camera (Kanneganti *et al.*, in preparation). Its initial science goals include variability studies of young stars, measurements of fundamental properties for low mass stars and brown dwarfs, observations of asteroids, and follow-up of carbon stars identified by 2MASS (VAIL 2005¹⁶). It saw first light in December 2004. The telescope has a focal plane scale of 16.92 seconds of arc (") millimeter (mm^{-1}) and a field-of-view 39.4 minutes of arc (')

¹⁶An on-line version of an informational poster that VAIL displayed locally is available <http://www.astro.virginia.edu/research/instrumentation/images/poster-20050406.jpg>

across (UVa 2006).¹⁷ When mounted on this telescope, FanCam has a 27.56'' mm⁻¹ scale and an 8.7' field-of-view (VAIL 2006).¹⁸ Table 5.1 describes the telescope and camera further, and Table 5.2 details some of the available filters.¹⁹ Figure 5.1 is a mechanical drawing illustrating some of the features of FanCam.

TABLE 5.1
CHARACTERISTICS OF THE FAN MOUNTAIN REFLECTOR AND CAMERA

Parameter		Description
Objective Size	(meters)	0.8
	(inches)	31
Optics		Classical Cassegrain
Telescope Focal Ratio		f/15.484
Telescope Effective Focal Length	(meters)	12.192
	(inches)	480.0
Telescope Focal Plane Scale	('' mm ⁻¹)	16.92
Focal Plane Array		Rockwell Hawaii-I HgCdTe
Focal Plane Array Description		thick, back-illuminated, coated
FanCam Field of View	(°)	8.7
Detector Size	(pixels)	1,024 x 1,024
Detector Pixel Size	(µm)	18.5
FanCam resolution	('' pixel ⁻¹)	0.5098
Detector Gain	(e ⁻ DN ⁻¹)	4.6
Detector Read Noise	(e ⁻ rms)	17
Optimal Detector Temperature	(K)	77

REFERENCES.—UVa 2006; VAIL 2006; Kanneganti *et al.* in preparation, S. Kanneganti 2006, private communication

¹⁷Telescope specifications maintained by UVa are available at
<http://www.astro.virginia.edu/research/observatories/31inch/31-specs.php>

¹⁸Instrument specifications maintained by VAIL are available at
http://www.astro.virginia.edu/research/instrumentation/firc_specs.php

¹⁹VAIL lists filter specifications on-line at
<http://www.astro.virginia.edu/research/observatories/FMOfilters.php#31inch> and
http://www.astro.virginia.edu/research/instrumentation/firc_specs.php

TABLE 5.2
CHARACTERISTICS OF SELECTED FILTERS

Filter ^a (2MASS Prototype)	Passband ^b (μm)	Central Wavelength (μm)	Limiting Magnitude ^c
J	1.105 – 1.395	1.250	19.0
H	1.515 – 1.817	1.666	18.0
K _S	2.045 – 2.335	2.190	17.0

NOTES.— ^aAdditional filters currently include K, Y, H₂, Br- γ , FE-II, Pa- β , and two polarizers. Future plans include the installation of a low-resolution prism plus medium- and high-resolution grisms.

^bPassbands were measured at room temperature by manufacturer.

^cLimiting magnitude is based on a 10- σ detection after 10 minutes of on-source observation.

REFERENCES.— Passbands are from VAIL 2006 and S. Kanneganti 2006, private communication. Limiting magnitudes are from Kanneganti *et al.*, in preparation.

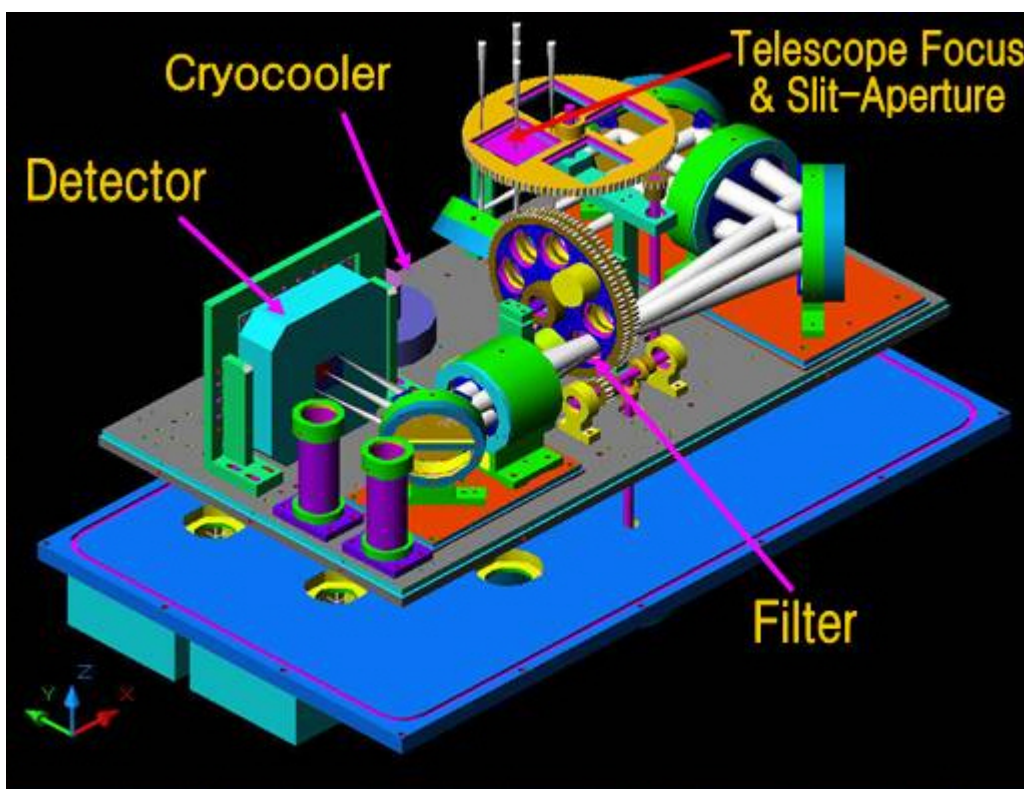


FIG. 5.1. — FanCam Mechanical Drawing. Image source: VAIL.

Plans for FanCam and the 31-inch reflector include the development of an autoguider. However, the telescope currently tracks the sky reliably for at least

30 seconds. Longer exposures are possible, but image motion will occasionally render an exposure useless. To observe objects of 17th magnitude or fainter, multiple short exposures are combined. For astrometric accuracy, the individual frames in the stacked exposure might need to be aligned within a fraction of a pixel. Appropriate plate constants may be able to account for large shifts or rotations but time-constraints prevented testing this technique. Therefore, observations for this study were limited to single exposures of 30 seconds or fewer.

The nightly pointing calibration of FanCam and the 31-inch reflector uses a known bright star positioned so that it is visible in the finder but does not impinge on the detector. This offset protects the sensitive focal plane array (FPA) in FanCam. However, it also introduces a small but uncertain offset between coordinates displayed by the telescope control system and the center of the field that the telescope is observing. This discrepancy can increase the difficulty of setting up and observing faint objects not visible in the finder.

5.3 ASTROMETRIC CALIBRATION REGION

Ideally, the astrometric quality testing and calibration of FanCam would have included the measurement of preliminary parallaxes and proper motions for several stars that have high-quality parallaxes observed at other facilities. However, selected stars from the *Catalogue of Stars with Proper Motions Exceeding 0.5" Annually* (Luyten 1979) were either too bright for 2-second exposures or too faint to be identified reliably with the current telescope pointing. Several early L dwarfs with spectroscopic

distance estimates (K. I. Cruz 2004, private communication) were too faint to observe using single 30-second exposures or too faint to be identified reliably.

During Fall 2005, FanCam was removed from the telescope to re-weld and refinish the vacuum seal surfaces (Kanneganti *et al.*, in preparation). While it was being serviced, a decision was made to use open clusters as astrometric calibration regions because several had been previously observed as part of other projects. NGC 2169 and NGC 2420 were selected as the best candidates based on the quality and quantity of frames available. Although many exposures were available, a significant number were taken at large hour angle and without careful positioning to ensure a consistent group of stars was visible. After FanCam was re-installed in November 2005, additional observations of these fields were made with the specific intention of using them as astrometric calibration regions.

Astrometric calibration probably should also consider all of the proposed filters, which for FanCam would include J, H, and K_S as described in Table 5.2. However, due to the limited observing time available during Fall 2005 and Spring 2006, only the frames taken with the J filter were included in this study. J-band has the advantage of reduced sky brightness compared to the other bands; it is the filter most likely to be used for a parallax program with FanCam. The USNO infrared parallax program observed L dwarfs in H band and T dwarfs in J band with similar precision in each filter.

During the reduction of the astrometric calibration regions, the selection of images was further narrowed to observations of NGC 2420 on three nights. Table 5.3

provides additional information about this cluster. Table 5.4 lists the frames selected.

Table 5.5 lists the twenty stars selected within this region for evaluation, which are also identified in Figure 5.2.

In a separate analysis, S. Kanneganti (2005, private communication) compared ninety stars from NGC 2420 frames with 2MASS images and determined that 51% of the FanCam stellar images were within 50 milliseconds of arc (mas), or 1.8 μm , of the 2MASS positions. However, for stars with K_s (2.159 μm according to Cohen, Wheaton, & Megeath 2003) magnitudes between 9 and 14, 2MASS positions are internally repeatable to within 40 to 50 mas and show residuals of 70 to 80 mas (Cutri 2005) when compared with the *USNO CCD Astrograph Catalog* (Zacharias *et al.* 2000, hereafter UCAC).

TABLE 5.3
PROPERTIES OF NGC 2420 FROM LITERATURE

Parameter	Value	Reference
Position (2000.0)	07 38 23 +21 34 24	1
Classification	Open Cluster	
Distance (pc)	2742	2
Proper Motion (mas yr^{-1})	4.3 \pm 0.3	3
Position Angle of Proper Motion (degrees)	198 \pm 5	3
Radial Velocity (km/s)	67 \pm 8	4
Age (years)	2.00 $\times 10^9$	2
Metallicity ([Fe/H])	-0.38 \pm 0.07	4

REFERENCES.—(1) Xin & Deng 2005; (2) Tadross *et al.* 2002; (3) Loktin & Beshenov 2003; (4) Friel *et al.* 2002;

TABLE 5.4
 CATALOG OF NGC 2420 FRAMES USED FOR ASTROMETRIC CALIBRATION

Observation Date	Frame	EST Time ^a (hh:mm)	Hour Angle ^b (minutes)	Exposure (seconds)	Seeing ^c (")	Shape ^d	Inadequate Stars ^e	Original Purpose ^f
2005-JAN-09	234	00:36	2E	2	2.0	skewed	1, 2, 3	Saturn
2005-JAN-09	235	00:36	2E	2	1.8	skewed	1, 2, 3	Saturn
2005-JAN-09	236	00:37	1E	2	1.5	slightly skewed	1, 2, 3	Saturn
2005-JAN-09	237	00:37	1E	2	1.8	oval	1, 2, 3	Saturn
2005-JAN-09	238	00:37	1E	2	2.0	roundish	1, 2, 3	Saturn
2005-JAN-09	239	00:37	1E	2	2.0	oval	2, 3	Saturn
2005-JAN-09	240	00:37	1E	2	2.0	skewed	2, 3	Saturn
2005-JAN-09	241	00:38	0	2	2.3	skewed	2, 3	Saturn
2005-JAN-09	242	00:38	0W	5	2.0	roundish	2, 3	Saturn
2005-JAN-09	243	00:38	0W	5	2.0	roundish	2, 3, 10	Saturn
2005-JAN-09	244	00:39	1W	5	2.0	round	2, 3	Saturn
2005-JAN-09	245	00:39	1W	5	2.0	roundish	1, 2, 3	Saturn
2005-JAN-09	246	00:39	1W	5	1.8	skewed	1, 2, 3	Saturn
2005-JAN-09	247	00:39	1W	5	1.8	fairly round	1, 2, 3	Saturn
2005-JAN-09	248	00:40	2W	5	2.0	skewed	1, 2, 3	Saturn
2005-JAN-09	249	00:40	2W	5	2.3	slightly oval	1, 2, 3	Saturn
2005-JAN-09	250	00:40	2W	5	2.3	slightly oval	1, 2, 3	Saturn
2005-JAN-09	251	00:41	3W	5	1.8	slightly oval	1, 2, 3	Saturn
2005-FEB-19	283	00:45	169W	5	1.5	skewed	1, 2, 3	Saturn
2005-FEB-19	284	00:47	171W	5	2.0	skewed	1, 3	Saturn
2005-FEB-19	285	00:48	172W	5	2.0	skewed	1	Saturn
2005-FEB-19	286	00:48	172W	5	2.0	skewed	1	Saturn

TABLE 5.4 (CONTINUED)
 CATALOG OF NGC 2420 FRAMES USED FOR ASTROMETRIC CALIBRATION

Observation Date	Frame	EST Time ^a (hh:mm)	Hour Angle ^b (minutes)	Exposure (seconds)	Seeing ^c (")	Shape ^d	Inadequate Stars ^e	Original Purpose ^f
2005-FEB-19	287	00:49	173W	5	1.9	skewed	1	Saturn
2005-FEB-19	288	00:49	173W	5	1.9	skewed	1	Saturn
2005-FEB-19	289	00:49	173W	5	2.0	skewed	1	Saturn
2005-FEB-19	290	00:49	173W	5	2.1	skewed	1, 3	Saturn
2005-FEB-19	291	00:49	173W	5	2.6	skewed	1, 2, 3	Saturn
2005-FEB-19	292	00:49	173W	5	1.9	skewed	1, 2, 3	Saturn
2005-NOV-19	403	03:46	13E	10	1.5	round	7	astrometry
2005-NOV-19	404	03:46	13E	10	1.8	round	7	astrometry
2005-NOV-19	405	03:46	13E	10	2.0	round	7, 17	astrometry
2005-NOV-19	406	03:47	12E	10	2.0	round	7, 10, 17	astrometry
2005-NOV-19	407	03:47	12E	10	1.8	roundish	7, 10	astrometry
2005-NOV-19	408	03:47	12E	10	1.8	slightly oval	7,	astrometry
2005-NOV-19	409	03:47	12E	10	1.8	round	7, 12,	astrometry
2005-NOV-19	410	03:48	11E	10	1.8	round	7	astrometry
2005-NOV-19	411	03:48	11E	10	1.0	skewed	1, 3, 7	astrometry
2005-NOV-19	412	03:48	11E	10	1.8	round	1, 7	astrometry
2005-NOV-19	423	03:53	6E	20	1.8	oval	1, 2, 3, 7, 12, 15	astrometry
2005-NOV-19	424	03:54	5E	20	1.8	round	1, 2, 3, 7, 12, 15	astrometry
2005-NOV-19	425	03:54	5E	20	2.2	round	1, 2, 3, 7, 12, 15, 17	astrometry
2005-NOV-19	426	03:55	4E	20	2.0	round	1, 3, 7, 12, 15, 17	astrometry
2005-NOV-19	427	03:55	4E	20	1.8	round	1, 3, 7, 12, 15	astrometry

TABLE 5.4 (CONTINUED)
 CATALOG OF NGC 2420 FRAMES USED FOR ASTROMETRIC CALIBRATION

Observation Date	Frame	EST Time ^a (hh:mm)	Hour Angle ^b (minutes)	Exposure (seconds)	Seeing ^c (")	Shape ^d	Inadequate Stars ^e	Original Purpose ^f
2005-NOV-19	428	03:55	4E	20	1.8	round	1, 7, 10, 12, 15	astrometry
2005-NOV-19	429	03:56	3E	20	1.8	skewed	1, 7, 12, 15	astrometry
2005-NOV-19	430	03:56	3E	20	1.8	round	1, 7, 12, 15	astrometry
2005-NOV-19	431	03:57	2E	20	1.5	round	1, 7, 12, 15	astrometry
2005-NOV-19	432	03:57	2E	20	1.5	slightly oval	1, 7, 12, 13, 15	astrometry
2005-NOV-19	443	04:05	6W	30	2.0	round	1, 2, 3, 7, 12, 15, 17	astrometry
2005-NOV-19	444	04:06	7W	30	2.6	oval	1, 2, 3, 7, 12, 15, 17	astrometry
2005-NOV-19	445	04:06	7W	30	1.8	slightly skewed	1, 3, 7, 12, 15	astrometry
2005-NOV-19	446	04:07	8W	30	2.0	round	1, 3, 7, 12, 15, 17	astrometry
2005-NOV-19	447	04:07	8W	30	1.5	round	1, 3, 7, 12, 13, 15	astrometry
2005-NOV-19	448	04:08	9W	30	1.8	fairly round	1, 2, 3, 7, 12, 15	astrometry
2005-NOV-19	449	04:08	9W	30	2.2	skewed	1, 2, 3, 7, 12, 15	astrometry
2005-NOV-19	450	04:09	10W	30	1.8	mostly round	1, 2, 3, 7, 12, 13, 15	astrometry
2005-NOV-19	451	04:10	11W	30	1.8	round	1, 2, 3, 7, 12, 15	astrometry
2005-NOV-19	452	04:10	11W	30	2.0	round	1, 2, 3, 7, 12, 13, 15 17	astrometry
2005-NOV-19	535	04:50	51W	10	1.3	round	7	sensitivity
2005-NOV-19	536	04:50	51W	10	1.5	round	7	sensitivity
2005-NOV-19	537	04:50	51W	10	1.5	round	7	sensitivity
2005-NOV-19	538	04:51	52W	10	0.9	round	7, 12, 15	sensitivity
2005-NOV-19	539	04:51	52W	10	1.2	round	7, 15	sensitivity
2005-NOV-19	540	04:51	52W	10	1.0	round	7, 12, 15	sensitivity

TABLE 5.4 (CONTINUED)
 CATALOG OF NGC 2420 FRAMES USED FOR ASTROMETRIC CALIBRATION

Observation Date	Frame	EST Time ^a (hh:mm)	Hour Angle ^b (minutes)	Exposure (seconds)	Seeing ^c (")	Shape ^d	Inadequate Stars ^e	Original Purpose ^f
2005-NOV-19	541	04:51	52W	10	1.0	round	7	sensitivity
2005-NOV-19	542	04:52	53W	10	1.2	round	7, 12	sensitivity
2005-NOV-19	543	04:52	53W	10	1.0	round	7, 15	sensitivity
2005-NOV-19	544	04:52	53W	10	1.8	round	7	sensitivity

NOTES.—^aEastern Standard Time (EST) of observations based on timestamp associated with digital file containing raw frame.

^bHour angle in minutes indicates how far east (E) or west (W) of the meridian NGC 2420 was midway through each exposure.

^cSeeing is estimated from the full-width at half-maximum (FWHM) of evaluation star 20 in each image.

^dShape is described based on the contours and overall appearance of evaluation star 20 in each image.

^eInadequate stars were dropped from individual frames for several reasons: missing, too close to an edge, saturated, or extremely misshapen.

^fMost frames used herein were not taken specifically for astrometric calibration (astrometry). The January and February frames were used for calibration during observations of the moons of Saturn. The frames taken late on November 19 were used to determine the limiting magnitudes of FanCam (C. Park 2006, private communication).

TABLE 5.5
ASTROMETRIC EVALUATION STARS SELECTED IN NGC 2420

Evaluation Star	2MASS Designation ^a	J (mag)	H (mag)	K _s (mag)	USNO-B1.0 Designation	NGC 2420 ID ^b
1	07380627+2136542	10.781 ± 0.021	10.198 ± 0.019	10.125 ± 0.018	1116-0164806	41
2	07381549+2138015	10.903 ± 0.021	10.405 ± 0.023	10.305 ± 0.018	1116-0164869	76
3	07382696+2138244	10.590 ± 0.021	10.057 ± 0.022	9.982 ± 0.018	1116-0164970	174
4	07382208+2136432	10.806 ± 0.022	10.277 ± 0.024	10.192 ± 0.020	1116-0164929	119
5	07382195+2135508	10.840 ± 0.024	10.350 ± 0.026	10.210 ± 0.020	1115-0161842	
6	07382687+2135460	11.987 ± 0.022	11.904 ± 0.022	11.861 ± 0.020	1115-0161940	172
7 ^c	07381507+2134589	8.572 ± 0.021	7.854 ± 0.016	7.687 ± 0.027	1115-0161730	
8	07382148+2135050	11.345 ± 0.022	10.805 ± 0.024	10.707 ± 0.018	1115-0161830	
9	07382984+2134509	11.107 ± 0.022	10.592 ± 0.022	10.475 ± 0.017	1115-0161983	192
10	07383760+2134119	10.848 ± 0.022	10.358 ± 0.024	10.234 ± 0.020	1115-0162073	236
11	07382936+2134309	12.049 ± 0.028	12.038 ± 0.030	11.946 ± 0.023	1115-0161978	190
12	07382166+2133514	9.5430 ± 0.024	8.954 ± 0.023	8.799 ± 0.018	1115-0161834	115
13	07382696+2133313	10.182 ± 0.022	9.772 ± 0.022	9.662 ± 0.017	1115-0161945	173
14	07382724+2133166	11.792 ± 0.022	11.331 ± 0.022	11.216 ± 0.018	1115-0161953	176
15	07382418+2132540	9.388 ± 0.021	8.721 ± 0.018	8.572 ± 0.018	1115-0161886	140
16	07381822+2132062	10.882 ± 0.022	10.413 ± 0.024	10.272 ± 0.018	1115-0161775	91
17	07382406+2132148	10.758 ± 0.029	10.279 ± 0.031	10.180 ± 0.026	1115-0161881	
18	07382935+2132375	11.784 ± 0.021	11.265 ± 0.022	11.183 ± 0.020	1115-0161977	
19	07382114+2131418	10.988 ± 0.022	10.524 ± 0.024	10.413 ± 0.017	1115-0161826	111
20 ^d	07382285+2134069	12.021 ± 0.021	11.490 ± 0.022	11.427 ± 0.017	1115-0161858	

NOTES.—^a2MASS designations are based on right ascension and declination (J2000) and have the form hhmmss.ss+ddmmss.s.

^bNGC 2420 identification follows the numbering in Cannon & Lloyd (1970).

^cAstrometric evaluation star 7 is also TYC 1373-01207-1 (Høg *et al.* 2000).

^dastroc and MPRP treated astrometric evaluation star 20 as the expected parallax star. The grading of frames is based on the quality of the image of this star.

REFERENCES.—Photometry is from 2MASS. USNO-B1.0 is Monet *et al.* (2003).

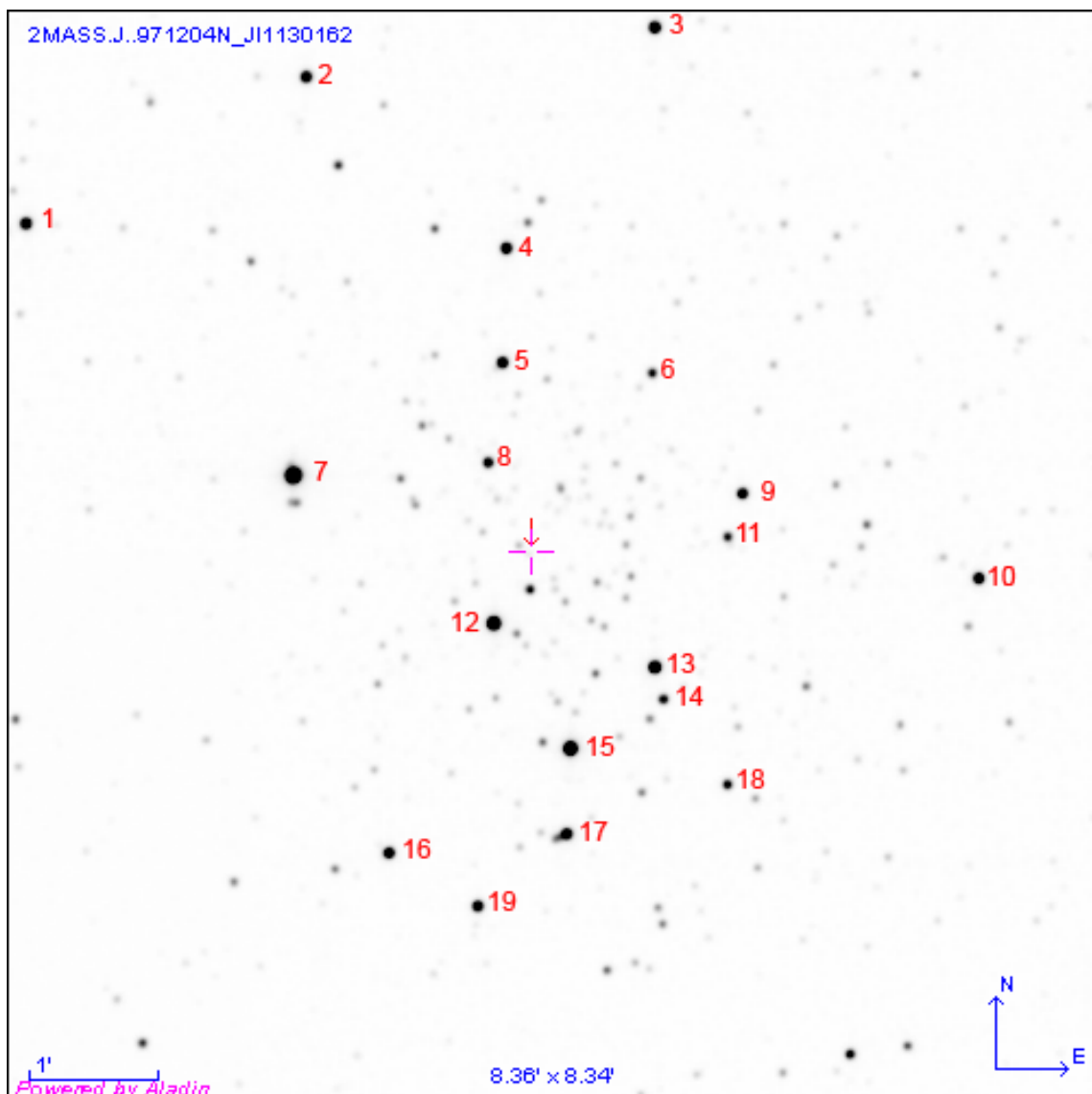


FIG. 5.2. — NGC 2420 with Astrometric Evaluation Stars Identified. Image Source: 2MASS J-band image taken 1997 April 17 via Aladin with annotations by J. L. Bartlett & J. L. Bartlett.

5.4 OBSERVATIONS AND ANALYSIS

Sixty-eight exposures of NGC 2420 taken with FanCam in January, February, and November 2005 using the J filter form the basis of this study. Exposure times ranged from 2 to 30 seconds. FanCam does not use a shutter. The custom imaging

software, *astrix* (A. Smith 2004, private communication), read out the FPA at the beginning and end of each exposure; *voodoo* (Leach & Low 2000; M. Nelson 2006, private communication) has now replaced *astrix*. The difference between those two read-outs was stored as the image in Flexible Image Transport System (FITS) format. No identifying or explanatory header information was included; observation times were later obtained from the computer time-stamp associated with the raw frames. Observations were made in batches. The telescope was moved slightly while each image was being read-out to provide manual dithering.

In November, a series of identical length exposures were also made close to the astrometric calibration field for use in estimating the sky background. Previously, the science images themselves were used to estimate the sky background.

When the sky was clear near sunset or sunrise, sky flats and dark exposures were also obtained for calibration purposes. Otherwise, the most recent sky flats and dark exposures were used for calibration.

The raw images (flats, darks, science images, and sky background images) were downloaded from the imaging computer in the 31-inch telescope control room or from a compact disc-read only memory (CD-ROM) produced on that machine. Then, rows 511 and 512 in all frames were replaced with pixels from rows 1,023 and 1,024 shifted by one column to the left using an Image Reduction and Analysis Facility (IRAF) routine (Tody 1986, 1993; hereafter IRAF²⁰) developed by C. Park (2005 & 2006, private communication); these rows are displaced during the read-out as shown in Figure 5.3 on

the following page. The current recommended reduction procedure is to treat these rows as bad pixels rather attempt to fix them (C. Park 2006, private communication). Next, all of the images were trimmed to eliminate bad columns and rows caused by misalignment of the camera with the focal plane aperture. VAIL has decided to leave these dark regions as they are for the time being (C. Park 2006, private communication).

Another IRAF routine developed by C. Park (2005 & 2006, private communication) was used to flatten images in batches of identical regions through identical filters with identical exposure times. This routine combined the flats, darks, and sky background frames into single representative images. The sky background frames had the same exposure length as the science frames that they would be used to flatten. The representative dark image was subtracted from the representative sky flat to produce a master flat. The representative sky image was subtracted from each science image. Then, the sky-subtracted science images were divided by the master flat image. Finally, previously identified bad pixels were fixed.

²⁰IRAF is distributed by the National Optical Astronomy Observatories, which are operated by the Association of Universities for Research in Astronomy, Inc., under cooperative agreement with the National Science Foundation.

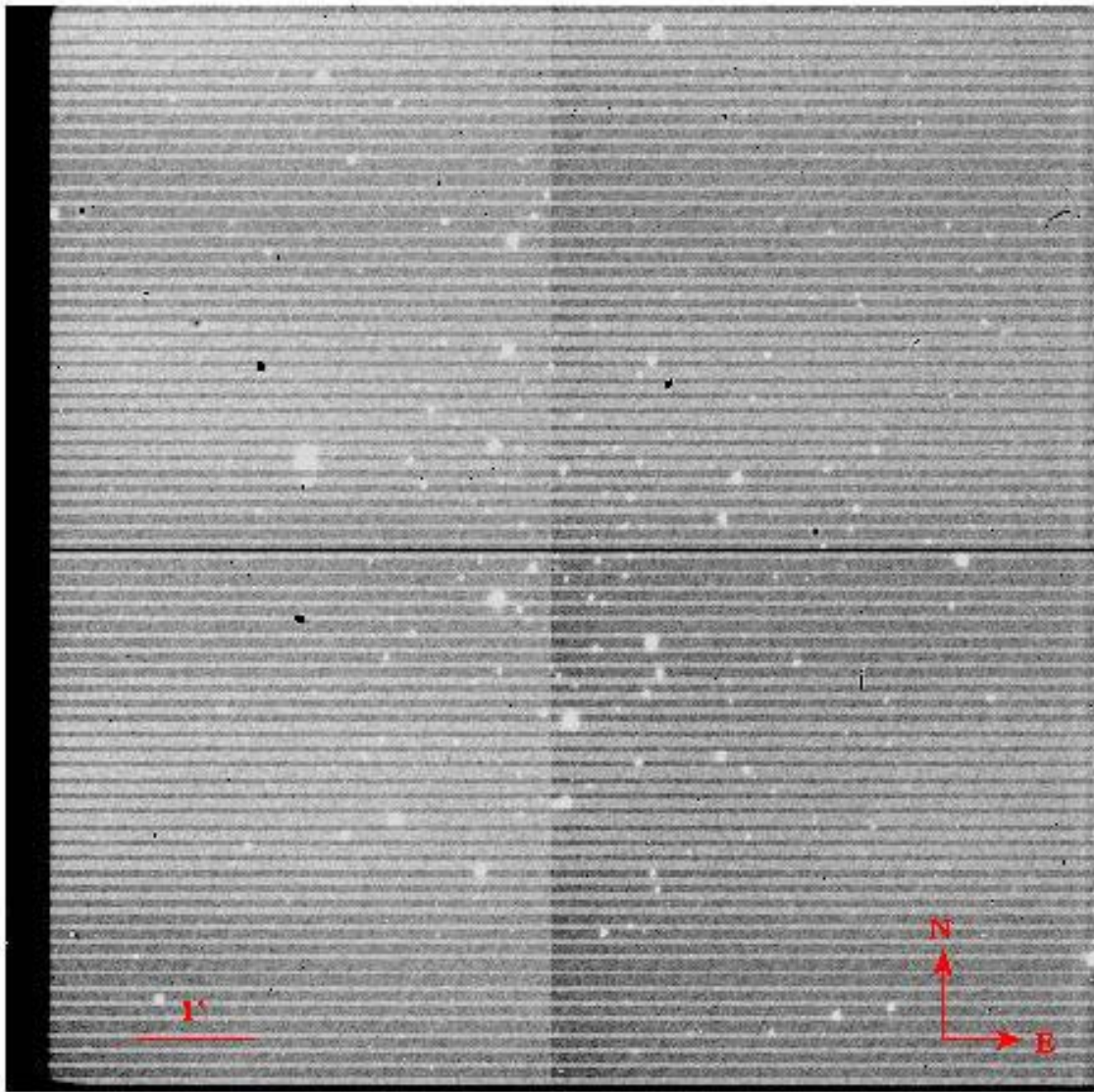


FIG. 5.3.—NGC 2420, Raw J-Band Frame 285 Taken 2005 February 19. In the middle of the frame, bad rows 511 and 512 can be seen. Misalignment of the detector and vacuum window caused the dark region along bottom and left side of the frame. Image Source: VAIL, O. Fox, & C. Park with annotations by J. L. Bartlett & J. L. Bartlett.

After this processing, the intensity of some pixels was negative, which is non-physical. Therefore, an appropriate constant was added to each pixel in a particular

image to bring the minimum value above zero. After this flattening procedure, the quality of the images was improved but visible structure remained in a number of images, as shown in Figure 5.4. However, samples of the sky background indicate this variation is significantly less than 1%. Furthermore, this type of artifact is rarely seen in FanCam images (C. Park 2006, private communication).

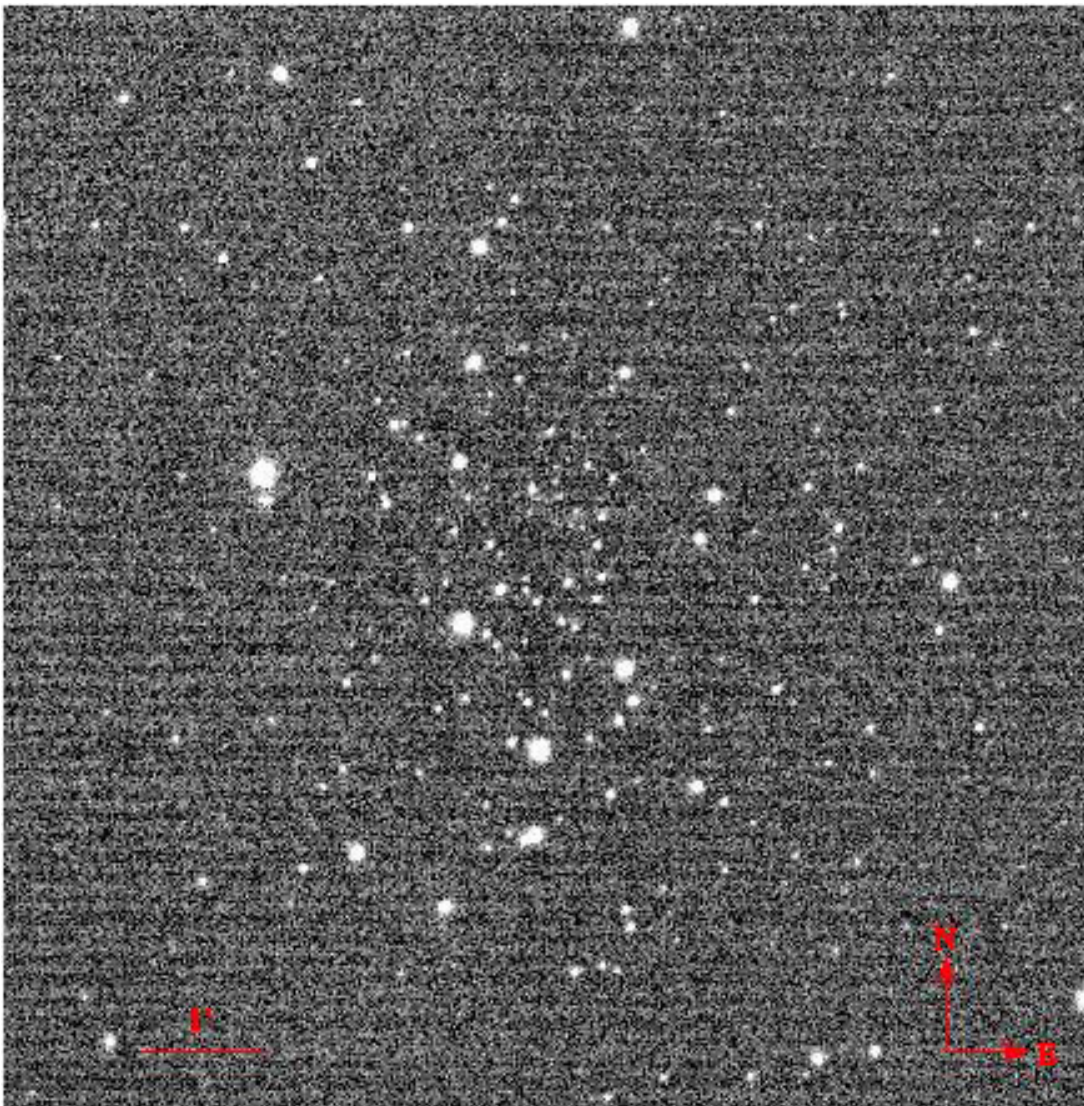


FIG. 5.4. — NGC 2420, Flattened J-Band Frame 285 Taken 2005 February 19. Some structure remains in the image after processing as described in section 5.4. Image Source: VAIL, O. Fox, & C. Park with processing by J. L. Bartlett & C. Park and annotations by J. L. Bartlett & J. L. Bartlett.

The flattened images were rotated so that north was to the top and east was to the left. The astrometric evaluation stars were checked individually for saturation and distortion. Then, Starlink conversion routines produced copies of the images in the format used by Figaro Version 2 (DST) for further processing using Figaro.

Begam, Ianna, and Patterson (2006, in preparation; hereafter BIP) describe the Figaro-based image reduction pipeline developed for the UVa Southern Parallax Program. Following these procedures, the images were cataloged and graded. The *astcor* routine extracted the position of each astrometric evaluation star. In frames where large constants had been added to ensure all pixels contained positive intensities, the constants had to be subtracted again in order for *astcor* to run properly.

Once positions for individual stars were measured, several combinations of images were considered: all images, individual nights, January and November images with moderate hour angles, and February and November images with large hour angles. Parallax input files (*pif*'s) were constructed for each case treating the central star, astrometric evaluation star 20, as the "parallax" star. For individual nights and for the February and November combination, the image with the best quality overall along with the image taken immediately after it were averaged to serve as the "trail plate." For the other combinations, four January images taken close to the meridian were averaged as the trail plate. Averaging several images increases the coordinate precision associated with the trail plate. The January trail plate lacked four astrometric evaluation stars so those stars were dropped from further analysis.

The McCormick Parallax Reduction Program (sager; hereafter MPRP) reduced the positions of the astrometric evaluation stars in each additional image to the selected trail plate. MPRP calculated a three plate-constant model to describe the mean positions of the astrometric evaluation stars

$$\begin{aligned}\varepsilon &= ax + by + c \\ \eta &= dx + ey + f\end{aligned}\tag{5.2}$$

where (x, y) are the coordinates of the astrometric evaluation stars in the system of their own image; (ε, η) are the coordinates of the astrometric evaluation star in the system of the trail plate; $a, b, c, d, e,$ and f are the plate constants that account for scale, orientation, and origin.

The mean error in a single observation of unit weight, estimated herein using the standard deviation of the plate adjustment model for each frame, is a measure of repeatability of positions. Table 5.6 lists the averages for each batch of frames considered; the x - and y -coordinates, which correspond to right ascension and declination, are considered separately. The errors range from 0.57 to 2.02 μm . The early November frames that were taken specifically as astrometric calibration frames have the smallest errors in x and y . The batches taken at large hour angles (February, November late, and both combined) have larger errors in y than x . The January frames taken within five minutes of the meridian have the largest errors, with its x -coordinate slightly worse than the y .

The precision for all frames considered is about $\pm 1.3 \mu\text{m}$, which is only slightly better than the single-position precision of $\pm 1.5 \mu\text{m}$ achieved for photographic plates. Charge-coupled device (CCD) images at the visible wavelengths should be repeatable

to nearly one-fiftieth (0.02) of a pixel (Monet *et al.* 1992), which translates to about $0.054 \mu\text{m}$ for FanCam. None of the batches evaluated approached this level of precision. The average mean error of unit weight for the Southern Parallax Program CCD Cousins V, R, and I (effective wavelengths 551.28, 654.82, and 816.10 nanometers, respectively) observations discussed in Chapter 3 is $0.41 \pm 0.11 \mu\text{m}$. The November images made within 15 minutes of the meridian come closest to this CCD program. However, photographic plates were the detector of choice for parallax programs throughout most of the twentieth century. Therefore, a parallax program should be possible using FanCam as well.

In comparison, USNO preliminary astrometric testing using cluster fields obtained mean errors of unit weight for a single observation of $\pm 7 \text{ mas}$ in J-band using a camera, IRCAM, that was not optimized for astrometry (Vrba *et al.* 2004). Their IRCAM results are better than approximately $\pm 40 \text{ mas}$ for FanCam frames overall or $\pm 19 \text{ mas}$ for the November frames taken within 15 minutes of the meridian. Encouraged by their IRCAM results, the USNO developed an infrared detector specifically for astrometry, ASTROCAM, with $27\text{-}\mu\text{m}$ pixels and a pixel resolution of $365.4 \text{ mas pixel}^{-1}$. Vrba *et al.* (2004) report preliminary parallaxes from ASTROCAM with average mean errors of unit weight of $15.5 \pm 4.9 \text{ mas}$, or $1.15 \pm 0.36 \mu\text{m}$, and $17.9 \pm 4.9 \text{ mas}$, or $1.32 \pm 0.36 \mu\text{m}$, in x and y respectively; these results are within the range achieved by FanCam. Better ASTROCAM results were achieved by using dithered triplets and by limiting the reference frame to the four brightest stars. Additional improvements in ASTROCAM precision were anticipated with the calculation of

parallaxes; the final solutions would include proper motions of the reference stars, differential color refraction (DCR), and the exclusion of frames with poor seeing.

5.5 DISCUSSION

The positions measured for the astrometric evaluation stars selected in NGC 2420 are similar in quality to those obtained for photographic plates but not as good as results achieved using CCD's in the visual and near-infrared bands. Therefore, the measurement of parallaxes using FanCam is possible. However, additional testing would be worthwhile before committing substantial amounts of observing time to a new infrared parallax program. Such testing should include the evaluation of possible higher-order plate constants, the analysis of stacked images, the assessment of the other proposed filters, and the measurement of an actual parallax. Astrometric improvements could be obtained by

- Increasing the number of exposures used, which should not be difficult using exposures shorter than 30 seconds
- Refining the initial image reduction process to obtain flatter images, which is expected as part of the continuing software development
- Optimizing the parallax reduction pipeline for use with infrared images and with the new hardware
- Installing the planned autoguider
- Modeling the atmospheric refraction so that DCR corrections may be included as necessary; although the effect should be small in the infrared, DCR corrections may improve measurements made at large hour angle

- Establishing appropriate astrometric observing procedures, including guidelines for grading frames

The results achieved with FanCam also indicate that a similar investigation of PAIRITEL may also be worthwhile. While PAIRITEL would have more limited time for astrometry, it is capable of detecting fainter objects than the smaller FanCam. With the probable loss of the USNO infrared parallax program, a need exists for another such program in the northern hemisphere. FanCam has an opportunity to meet this need.